Real-time spatial–spectral interference measurements of ultrashort optical pulses

D. Meshulach, D. Yelin, and Y. Silberberg

Department of Physics of Complex Systems, The Weizmann Institute of Science, Rehovot 76100, Israel

Received January 31, 1997; revised manuscript received March 27, 1997

Real-time linear spectral interference measurements of ultrashort pulses are shown experimentally. The technique involves measurements of the two-dimensional interference pattern of the spectral interference between a reference and a signal pulse propagating at an angle with respect to each other. No postprocessing is needed to extract the spectral phase difference between the two pulses. Quadratic spectral phase distortions as well as spectral phase discontinuities are measured. The method is applicable to single-shot measurements of ultraweak pulses and is useful for identification of the critical adjustments of ultrashort pulse shapers and compressors. © 1997 Optical Society of America [S0740-3224(97)02808-7]

1. INTRODUCTION

In recent years there has been rapid progress in the development of techniques for complete characterization of ultrashort pulses. Early methods, such as second-harmonic-generation intensity and interferometric autocorrelations,[1,2] provide information about the temporal amplitude but incomplete or no information about the phase. Recently several techniques were developed for complete characterization of the field of ultrashort pulses. The method of frequency-resolved optical gating[3–5] has been studied in several variants and has proved useful for obtaining the complete spectral phase and amplitude of ultrashort pulses by employing iterative algorithms to the measured data set. The technique of direct optical–spectral phase measurement[6] has been demonstrated, and recently it was extended to the measurement of discontinuities in the spectral phases of such pulses.[7] However, these techniques for complete characterization of ultrashort pulses require a nonlinear process and are therefore inherently limited to the measurement of relatively high-power pulses.

In many experimental situations there is a need to characterize a pulse modified by transmission through an optical system. This optical system could be as simple as a slab of dispersive material, or it could be an entire setup of optical elements, such as pulse stretchers–compressors. In these situations an initial high-intensity well-characterized pulse is available. Recently a measurement of ultraweak, ultrashort pulses was demonstrated that combined a frequency-resolved optical gating technique and a spectral interference (SI) technique.[8] The frequency-resolved optical gating technique, which involves a nonlinear process, was used independently to characterize the spectral phase of a short reference pulse, and the SI technique, which involves a linear measurement, was then used to measure the spectral phase difference between this pulse and an unknown signal pulse. Briefly, the SI technique, introduced by Froehly and colleagues[9,10] and Lepetit *et al.*,[11] involves a linear measurement of the spectral interference of two collinear pulses delayed in time by τ with respect to each other. This measurement yields the spectral phase difference $\varphi_{\mathrm{sig}}(\omega) - \varphi_{\mathrm{ref}}(\omega) - \omega\tau$, where $\varphi_{\mathrm{sig}}(\omega)$ and $\varphi_{\mathrm{ref}}(\omega)$ are the spectral phases of the unknown signal and reference pulses, respectively, and ω is the angular frequency. Because the power spectrum of the signal pulse can be measured, and $\varphi_{\mathrm{ref}}(\omega)$ and τ are known, $\varphi_{\mathrm{sig}}(\omega)$ can be extracted and the complex temporal field can be recovered by an inverse Fourier transformation. Usually the spectral phase difference between the signal and the reference pulses is extracted by postprocessing of the measured spectral interference signal, and unwrapping of the phase is required.

In this paper we demonstrate real-time spectral interference measurements of ultrashort pulses by an extension of the SI technique[12,13] which can be discussed within the framework of spectral holography.[14] Our scheme of spatial–spectral interference (SSI) involves two-dimensional measurement of the spectral interference between a reference pulse and a signal pulse propagating at an angle with respect to each other. The frequency components of the optical fields of the two propagating pulses are mapped in one dimension by a diffraction grating and a cylindrical lens and interfere at the focal plane of the lens. The cylindrical lens does not affect the propagating fields in the perpendicular direction, so interference fringes are formed. As in SI, SSI involves measurement of the spectral phase difference between a reference pulse and a signal pulse, so complete characterization of an unknown pulse requires a characterized reference pulse. Both SI and SSI techniques involve the use of a carrier signal for encoding of the spectral information. In SI, a delay between the two pulses is needed as a spectral carrier for the spectral phase information. In SSI, the spatial interference pattern, controlled by the angle of intersection between the two propagating fields,

0740-3224/97/0802095-04$10.00

can be interpreted as a spatial carrier for the spectral phase information. However, the use of a SSI technique removes some of the difficulties associated with SI. In particular, no delay between the reference and the signal pulses is required, and no postprocessing is needed to remove its effect. Furthermore, the spectral phase difference distribution, as well as its sign, is directly observed in real time, and no unwrapping of the spectral phase difference is needed. We demonstrate the SSI technique by measuring small and large quadratic dispersions of optical flats and by measuring the π phase jumps of a $0-\pi$ crafted pulse.

2. THEORY

Consider the geometry of Fig. 1, where a reference pulse $e_{\mathrm{ref}}(t)$ and a signal pulse $e_{\mathrm{sig}}(t)$ are propagating at an angle 2θ with respect to each other and impinging upon a diffraction grating. The grating and the cylindrical lens map the optical frequencies of the pulses at the focal plane of the lens along a direction perpendicular to the grating grooves, denoted x. The field along the perpendicular direction, y, is not affected. The two-dimensional interference intensity, $I(x, y)$, at the focal plane of the cylindrical lens is given by

$$\begin{aligned} I(x, y) &= |E_{\mathrm{ref}}(x_\omega)\exp[i\phi_{\mathrm{ref}}(x_\omega)] \\ &\quad \times \exp[ik(x_\omega)(f\cos\theta + y\sin\theta)]A(y) \\ &\quad + E_{\mathrm{sig}}(x_\omega)\exp[i\phi_{\mathrm{sig}}(x_\omega)] \\ &\quad \times \exp[ik_x(f\cos\theta - y\sin\theta)]A(y)|^2 \\ &= A^2(y)\{E_{\mathrm{ref}}{}^2(x_\omega) + E_{\mathrm{sig}}{}^2(x_\omega) \\ &\quad + 2E_{\mathrm{ref}}(x_\omega)E_{\mathrm{sig}}(x_\omega)\cos[\phi_{\mathrm{sig}}(x_\omega) - \phi_{\mathrm{ref}}(x_\omega) \\ &\quad - 2k(x_\omega)y\sin\theta]\}. \end{aligned} \tag{2.1}$$

Here $E_{\mathrm{sig}}(x_\omega)$ and $E_{\mathrm{ref}}(x_\omega)$ are the spectral amplitudes of the signal and the reference pulses, respectively, mapped onto the x direction; $\phi_{\mathrm{sig}}(x_\omega)$ and $\phi_{\mathrm{ref}}(x_\omega)$ are the corresponding spectral phases, and k is the wave-vector magnitude. The subscript ω is included to emphasize the mapping of the optical frequencies onto the x axis. The focal length of the lens is f, and $A(y)$ accounts for the intensity distribution in the y direction at the focal plane, assumed to be identical for both pulses.

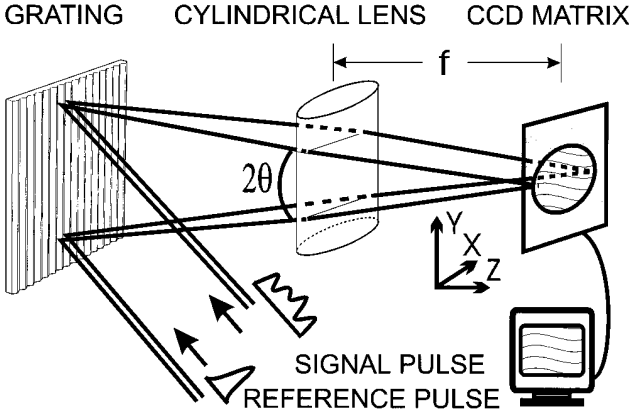

Fig. 1. Experimental arrangement for real-time SSI measurements. The reference and the signal pulses propagate at an angle 2θ with respect to each other. The spectra of the two pulses interfere at the focal plane of the cylindrical lens, where a CCD matrix is placed.

It is evident from Eq. (2.1) that, at any location x_ω, the fringes in the y direction have a sinusoidal pattern, shifted along y by the spectral phase difference between the relevant frequency components. Therefore any of the fringes traces the spectral phase difference between the two pulses as a function of the frequency. Furthermore, the interference pattern provides a natural phase scale because the fringe spacing along y, for any frequency, corresponds to a 2π phase shift. The angle between the two propagating pulses, which determines the fringe spacing along the y direction, behaves as a spatial carrier for the spectral information. It is also evident that the fringe contrast is maximized when the spectral amplitudes of the pulses are equal.

3. EXPERIMENTAL RESULTS

The experimental setup, shown in Fig. 1, consists of a diffraction grating, a cylindrical lens, a CCD matrix, and a monitor. The spectra of the two pulses, propagating at an angle $2\theta = 0.5°$ with respect to each other, interfere at the focal plane of the cylindrical lens, where a CCD matrix is placed. A diffraction grating with 600 grooves/mm and a cylindrical lens with a 25-mm focal length and an f-number of 1.3 were used to accommodate a bandwidth of 105 nm over the CCD width. At the focal plane each spectral component was focused down to $\sim 25\ \mu$m, and the CCD pixel size was $\sim 10\ \mu$m. The laser source for the experiment was a Ti:sapphire laser with an average power of 100 mW, 20-fs sech pulses centered at a wavelength of 805 nm, and a FWHM bandwidth of 56 nm. The laser beam was split into two by a thin, low-dispersion beam splitter. One part served for the reference pulses and the other for the signal pulses. In what follows, we describe several measurements of phase distortions that were imposed upon the signal pulses.

First we recorded the interference pattern of the signal and the reference pulses when no distortion was introduced. The results are shown in Fig. 2. Figure 2(a) corresponds to the case when the two pulses coincide in time (zero delay). Note that the fringe pattern is slightly wedged because the horizontal axis corresponds to frequency, and therefore the fringe spacing varies linearly. In Fig. 2(a) a small curvature of the fringes can be observed, which corresponds to some residual dispersion of our optics. A delay between the pulses corresponds to a linear spectral phase shift, which introduces a tilt to the interference pattern. This effect is clearly seen in Figs. 2(b) and Fig. 2(c) where positive and negative delays, respectively, of 333 fs were introduced between the pulses.[15] The delay between the pulses can be directly computed from the fringe pattern, $\tau(\omega') = (\partial\phi/\partial\omega)|_{\omega=\omega'}$. Our calculations based on the fringe pattern gave a delay of 331 fs, an excellent estimate of the induced delay. Note that the direction of the tilt uniquely determines the temporal relation between the signal and the reference pulses.

To demonstrate real-time display and measurements of spectral phase distortions, first we placed six fused-silica

glass optical flats, with a total thickness of 5.72 cm, in the signal beam. The interference pattern in this case is shown in Fig. 3(a). The parabolic fringes correspond to the quadratic spectral phase difference between the pulses. The measurements yielded a quadratic dispersion coefficient of $\phi'' = 354\ \mathrm{fs}^2/\mathrm{cm}$ for the fused-silica glass, in excellent agreement with the calculated value of $357\ \mathrm{fs}^2/\mathrm{cm}$ obtained with Sellmeir's coefficients as given by the glass's manufacturer. The interference pattern of the same two pulses, where a delay of 333 fs was introduced between them, is shown in Fig. 3(b). This delay introduces an additional linear term to the quadratic spectral phase. It is important to emphasize that the sign of the spectral phase difference is obvious from the curvature of the fringes. Placing the optical flats in the reference beam resulted in an inverted interference pattern. Note also that the full spectral phase difference is obtained. Next, we placed a 28.28-cm block of BK-7 glass in the signal beam. The resulting interference pattern is shown in Fig. 3(c). The measurements yielded a quadratic dispersion coefficient of $\phi'' = 452\ \mathrm{fs}^2/\mathrm{cm}$, in excellent agreement with calculations based on BK-7 glass data, which give $442\ \mathrm{fs}^2/\mathrm{cm}$. Note that some blurring occurs close to the edges, mainly caused by the aberrations of the cylindrical lens, which was not corrected for any aberration. Therefore for these calculations we used only the central part of the pattern.

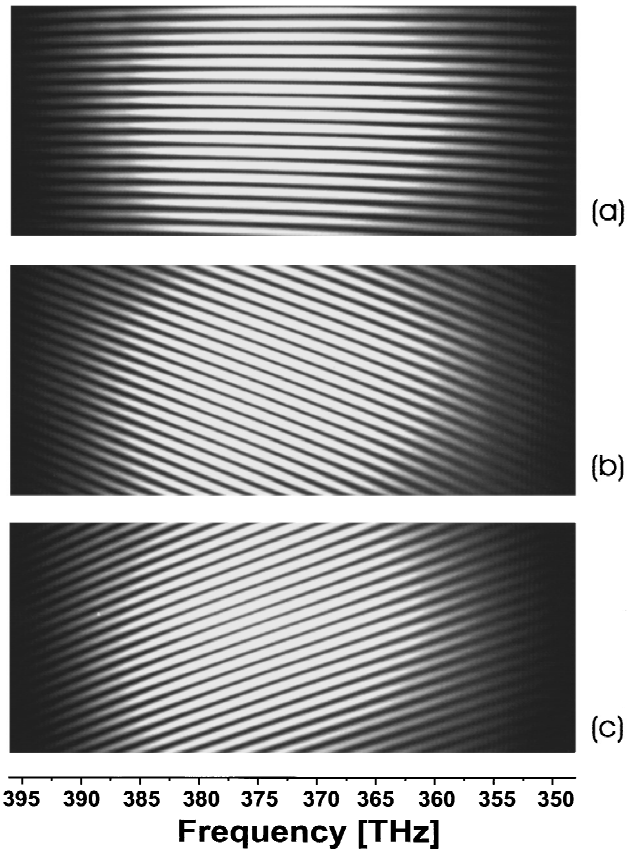

Fig. 2. Interference pattern of the spectrally dispersed signal and the reference pulses with no spectral phase distortion. (a) No delay between the pulses. (b) Delay of 333 fs between the pulses. (c) Delay of −333 fs between the pulses.

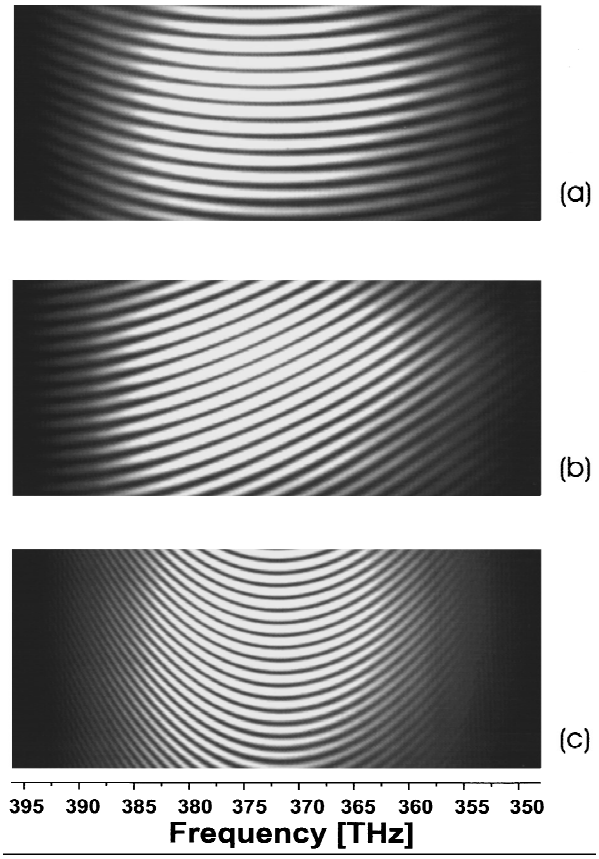

Fig. 3. Interference pattern of the spectrally dispersed signal and the reference pulses when optical glasses were inserted in the signal beam. (a) 5.72 cm of fused-silica glass; no delay between the pulses. The parabolic fringes correspond to the quadratic dispersion of the glass. (b) Same as (a), with a delay of 333 fs between the pulses. (c) 28.28 cm of BK-7 glass; no delay between the pulses.

Finally, to demonstrate that SSI is capable of locating and measuring spectral phase discontinuities, as in SI,[11] we constructed a folded $4f$ pulse shaper in the signal beam to craft $0-\pi$ pulses by a method similar to that reported in Ref. 7. Briefly, we inserted two microscope cover slips, each slip covering half of the spectrum in the pulse shaper, permitting the introduction of a controlled phase discontinuity to the spectral phase. The discontinuity of the spectral interference fringes, shown in Fig. 4(a), clearly demonstrates not only the π phase jump but also its location. Removing one of the cover slips introduced a time delay between the two regions of the signal spectrum, in addition to a π phase jump. Consequently, horizontal fringes are formed on one half of the interference pattern, and tilted fringes on the other, as is evident from Fig. 4(b).

4. CONCLUSIONS

We have shown that the SSI method, which is an extension of the SI method, can be used for measurement of the spectral phase difference between a reference pulse and a signal pulse. Complete characterization of an unknown pulse is possible in the case when an adequate reference pulse is available. In SI, a delay between the two pulses

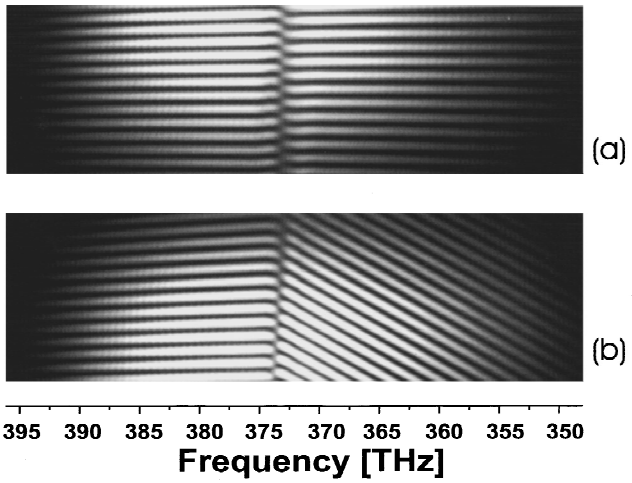

Fig. 4. Measurements of a π spectral jump. (a) Spectral phase jump resulting from a π discontinuity in the spectral phase. (b) A π jump and an additional time delay of half of the spectrum.

is needed as a spectral carrier for the spectral phase information. In SSI, the spatial interference pattern can be interpreted as a spatial carrier for the spectral phase information. However, the use of SSI is advantageous over the use of SI: Because no delay between the reference and the signal pulses is required, no postprocessing is needed for extraction of the spectral information. Furthermore, in SSI the spectral phase difference distribution, as well as its sign, is directly observed in real time, so unwrapping of the spectral phase difference is not needed. As in SI, SSI involves a linear detection of the fields, and therefore extremely weak pulses can be measured. In our setup the 100-mW laser beam was attenuated by 7 orders of magnitude. Single-shot measurements should also be possible with this technique.

Finally, we note that we have found this method extremely useful for optimizing various setups, such as pulse shapers and compressors. The fringe patterns, such as in Figs. 2–4, are displayed in real time, and the information is encoded in a most simple and easy-to-interpret pattern. The effect of various adjustments of the optical components on the signal pulse is displayed in real time, and the removal of phase distortions is greatly simplified.

In summary, we have demonstrated real time spectral measurements of weak ultrashort pulses. We did this by measuring small and large quadratic spectral phase distortions as well as $0 - \pi$ spectral phase discontinuities. SSI is applicable to measurements in low-repetition-rate and single-shot pulse systems. This characteristic should be extremely important in amplified short-pulse systems.

ACKNOWLEDGMENT

The authors thank D. Leibovitz, J. Chopen, J. Leibovitz, and Y. Kruvi for excellent technical support.

REFERENCES

1. M. Maier, W. Kaiser, and J. A. Giordmaine, Phys. Rev. Lett. **17**, 1275 (1966).
2. J. M. Diels, J. J. Fontaine, I. C. McMichael, and F. Simoni, Appl. Opt. **24**, 1270 (1985).
3. D. J. Kane and R. Trebino, Opt. Lett. **18**, 823 (1993).
4. R. Trebino and D. J. Kane, J. Opt. Soc. Am. A **10**, 1101 (1993).
5. T. Tsang, M. A. Krumbügel, K. W. DeLong, D. N. Fittinghoff, and R. Trebino, Opt. Lett. **21**, 1381 (1996).
6. K. C. Chu, J. P. Heritage, R. S. Grant, K. X. Liu, A. Dienes, W. E. White, and A. Sullivan, Opt. Lett. **20**, 904 (1995).
7. K. C. Chu, J. P. Heritage, R. S. Grant, and W. E. White, Opt. Lett. **21**, 1842 (1996).
8. D. N. Fittinghoff, J. L. Bowie, J. N. Sweetser, R. T. Jennings, M. A. Krumbügel, K. W. DeLong, R. Trebino, and I. A. Walmsley, Opt. Lett. **21**, 884 (1996).
9. C. Froehly, A. Lacourt, and J. C. Vienot, J. Opt. (Paris) **4**, 183 (1973).
10. J. Piasecki, B. Colombeau, M. Vampouille, C. Froehly, and J. A. Arnaud, Appl. Opt. **19**, 3749 (1980).
11. L. Lepetit, G. Chériaux, and M. Joffre, J. Opt. Soc. Am. B **12**, 2467 (1995).
12. A. P. Kovács, K. Osvay, Zs. Bor, and R. Szipöcs, Opt. Lett. **20**, 788 (1995).
13. K. Misawa and T. Kobayashi, Opt. Lett. **20**, 1550 (1995).
14. A. M. Weiner, Prog. Quantum Electron. **19**, 161 (1995).
15. A. M. Weiner, D. E. Leaird, D. H. Reitze, and E. G. Paek, IEEE J. Quantum Electron. **28**, 2251 (1992).